Journal of Experimental and Computational Methods in Applied Sciences, pp. 1–17

Comparative Frameworks for Next- and Third-Generation Sequencing in Genomic Applications

Fouad Idrissi [1], Sameh Saber [2], Marwa Ahmed Nakhriry [3]

1. *Université Méditerranéenne de Casablanca, Boulevard Zerktouni No. 11, Casablanca, Morocco*
2. *Department of Pharmacology, Delta University for Science and Technology*
3. *Beni-suef university, 34M2+5X5, Qism Bani Sweif, Beni Suef, Beni Suef Governorate 2722165, Egypt*

Abstract

Next-generation sequencing transformed genomics by shifting from capillary separations to massively parallel molecular imaging, while third-generation platforms extended read lengths and enabled direct sensing of native nucleic acids. Against this historical backdrop, technical choices now revolve around chemistryphysics trade-offs, error models, and computational inference rather than a single dominant instrument class. This paper develops a comparative, methods-focused analysis of the dominant architectures, including sequencing-by-synthesis with cyclic fluorescent interrogation and single-molecule modalities that detect polymerase-mediated incorporations or ionic-current perturbations through nanometer pores. Assay steps from library construction to basecalling are treated as a coupled stochastic pipeline whose performance hinges on fragment length distributions, molecular tagging, transduction bandwidth, and priors embedded in learning-based decoders. A unified modeling view is proposed for coverage, assembly continuity, and haplotype resolution across variant scales, relating platform-specific error spectra to algorithmic robustness in consensus, phasing, and structural discovery. Special attention is given to epigenetic and transcriptomic readouts, where native modification detection and full-length isoform capture yield qualitatively new observables that cannot be retrofitted from short fragments alone. Economic and operational considerations are formalized through throughput and cost functions that incorporate flowcell physics, pore occupancy, polymerase kinetics, and sample complexity. By mapping the tensions between accuracy and contiguity, speed and depth, and standardized pipelines and bespoke analyses, the paper articulates design implications for population sequencing, clinical validation, and multi-omic integration. The resulting framework clarifies when short-read depth remains optimal, when long-read continuity is decisive, and how hybrid and adaptive strategies best exploit the strengths of both generations.

Introduction

High-throughput sequencing is best understood as an engineered pipeline in which biochemical preparation, nanoscale transduction, and statistical inference jointly determine what biological statements can be defended [1]. Rather than attributing outcomes to read length alone, the disciplined view treats each platform as a signal-processing system with identifiable transfer functions, noise sources, and regularizers. Library molecules provide the priors and boundary conditions; the instrument instantiates a measurement operator corrupted by stochastic kinetics, optical cross-talk, or ionic turbulence; downstream software inverts that operator with denoisers, aligners, and decoders that encode assumptions about genomes and transcriptomes. From this vantage, basecalling becomes a supervised estimation problem with domain shift, alignment becomes a structured search over graph indices, and variant calling becomes Bayesian decision-making under coverage- and context-dependent uncertainty; however, none of these stages can be optimized in isolation because upstream choices reshape the data manifold presented to downstream algorithms. Within cyclic, clonal next-generation sequencing (NGS), the physics is set by synchronized chemistry repeated thousands of times per cluster. Each incorporation event generates photons that must be collected with sufficient numerical aperture, discriminated across color channels, and demultiplexed across densely packed features. Misincorporation and phasing errors accumulate as some strands lag or lead the cohort; the distribution of cycle-dependent quality scores often drifts with local GC content, secondary structure, and reagent aging. Flow-cell surface chemistry and bridge amplification modulate cluster density, which itself trades off against optical bleed-

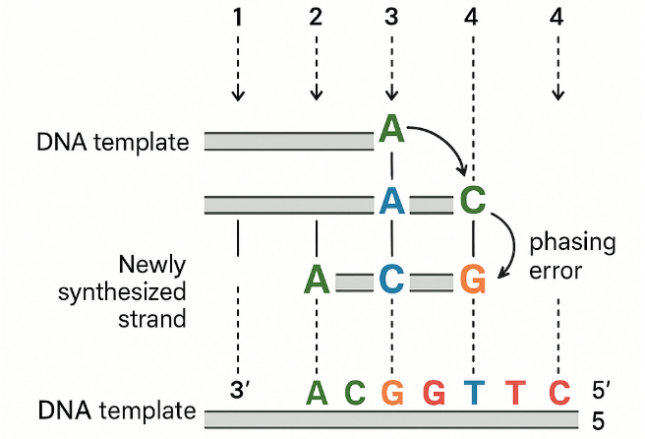

Figure 1: Phasing Errors in Cyclic NGS Sequencing

through and deconvolution stability [2]. Sequencers that use reversible terminators add further structure: blocking group removal kinetics create temporal correlations in noise that violate naïve independence assumptions. The result is a per-cycle, per-context error process that is low in magnitude but high in structure, and which bioinformatic tools exploit when modeling context-aware quality recalibration or read trimming. The point is not that errors are rare; it is that they are predictable enough to be modeled, which is why depth aggregates into trustworthy consensus under realistic coverage budgets.

Single-molecule platforms reconfigure the measurement equation. In polymerase-mediated real-time systems, interpulse duration and pulse width report on the kinetic landscape of the active site, while in nanopore systems, discrete ionic current levels and dwell times summarize the joint state of k-mers, motor enzyme, and pore geometry. The raw error rate is higher, but so is the contextual support: a single molecule provides tens to hundreds of kilobases of correlated signal, and modified nucleotides perturb the observable in ways that can be learned. Training a basecaller then resembles solving a conditional density estimation task with structured latent variablesmotifs, methylation patterns, and device-specific drift [3]. On the other hand, the heavy-tailed error modes of single-molecule data impose nontrivial demands on consensus algorithms; chimeric reads, polymerase stalls, and pore blockages produce outliers that are not well captured by Gaussian or simple binomial models. Long-range redundancy through circular consensus or multi-coverage assemblies acts as an error-shaping code in the information-theoretic sense, reassigning uncertainty from per-base noise to rare mis-joins whose consequences are more severe but easier to diagnose.

Error and coverage statistics anchor these observations in quantifiable terms. Classical LanderWaterman calculations characterize the expected uncovered fraction as a function of read length and depth under a Poisson assumption; departures from Poissonarising from amplification bias, fragmentation nonuniformity, or sequence-dependent mappabilitydistort those expectations. GC extremes impose multiplicative biases that persist despite optimized polymerases and buffer systems, and duplication rates inflate apparent depth without increasing evidence. Coverage models that incorporate fragment length distributions and mappability masks predict callable genome fraction more faithfully than scalar depth metrics. In metagenomes, the relevant quantity is not merely coverage but its allocation across taxa with widely varying abundance, where negative binomial dispersion and index hopping contribute identifiable confounders [4]. A practical aside: reagent barcoding strategies create low-frequency cross-sample contamination that is invisible to average coverage yet disastrous for pathogen detection thresholds if not explicitly modeled in the prior.

Library preparation is the first and most consequential act of modeling. Fragment size distribution sets the scale at which repeat structures can be bridged; enzymatic fragmentation reshapes sequence context around breakpoints; end-repair and ligation efficiencies introduce sequence-dependent survivorship that propagates into mappability differences. Uracil-DNA glycosylase treatment reduces deamination artifacts in ancient or formalin-fixed samples but removes authentic signal from deaminated cytosines when the scientific question is damage profiling. Choice of adapters encodes not only indices but also the handles that later informational steps use for error detection and rescue. For long-read platforms, ligation versus transposase tagmentation determines whether nicked or damaged molecules survive into the pore, which in turn changes the read length tail and the stability of the motor enzyme. For RNA, capture protocols set the operational definition of a transcript: random priming, poly(A) selection, or ribodepletion each specifies a distinct sampling operator that the quantifier must invert [5]. When variant callers ingest these signals, their priors on local haplotype complexity, ploidy, and sequencing error are calibrated by exactly these preparation decisions; the same tumor biopsy can look clonally stable or wildly heterogeneous depending on whether unique molecular identifiers were used to collapse PCR duplicates in a damage-aware model, which is not a mere implementation detail.

Assembly and polishing make these abstractions concrete. In short-read landscapes, de Bruijn graphs factor genomes into k-mers whose multiplicities encode copy number and repeats; k must be long enough to disambiguate repeats yet short enough to maintain connectivity through coverage dips. Error correction converts the k-mer spectrum from a mixture to a near-discrete distribution, after which unitigs form; scaffolding with mate-pairs, optical maps, or proximity ligation adds long-range constraints that convert graphs into linearizations punctuated by unresolved repeats. For long-read datasets, string graphs or laysers of overlap assembly recover more of the true structure, but their success hinges on robust detec-

tion of spurious overlaps generated by systematic errors in homopolymers and low-complexity tracts. Though consensus polishers trained on platform-specific error modes can remove most indel noise, they can also hallucinate k-mer corrections when the training distribution does not match the organism of interest, as seen in AT-rich extremophiles. Repeat families such as segmental duplications and centromeric satellites remain chokepoints where the asymmetry between read length and repeat size governs contiguity; the emergence of pangenome graph references proposes to absorb this complexity into the reference itself, yet that transfer of difficulty from assembly to alignment is not obviously a universal improvement. [6]

Variant detection inherits both the generative and the combinatorial burdens. Single-nucleotide variants and small indels are judged against a local haplotype graph with likelihoods aggregated across reads; when contexts are repetitive or diploid assumptions fail, likelihoods flatten and posterior confidences lag. Structural variants require long-range cuessplit read signatures, discordant pair orientations, read depth plateaus, and assembly-based reconstructionsto reach adequate sensitivity at balanced precision. Phasing, for its part, is less a luxury than a structural property: without phase, compound heterozygosity, cis-regulatory architectures, and drug metabolism genotypes cannot be resolved. Trio-aware phasing, Strand-seq, and statistical imputation extend block lengths in different ways, and long-read or linked-read data provide physical scaffolds on which phasing algorithms can climb. High-ploidy plant genomes introduce further complications by making the state space of genotypes explode; priors on allele dosage, subgenome divergence, and homeologous exchange must be encoded explicitly or the caller degenerates into noise. A digression that appears orthogonal at first glancethe freezer dwell time of blood prior to plasma separationturns out to modulate cell-free DNA fragmentomes and thus the detectability of minimal residual disease, a dependency easily missed unless the lab protocol is treated as part of the model; however, the best callers will still fail in regions where the reference is itself a poor scaffold for biological diversity. [7]

Transcriptome profiling exposes the coupling between chemistry and statistics yet again. Short-read RNA-seq generates read clouds that only indirectly observe isoform structure; quantification relies on probabilistic assignment of ambiguous fragments to a transcriptome that is itself incomplete. Effective lengths, sequence-specific biases, and $3'$ end enrichment define the feasible set of inferences, while allelic imbalance and nonsense-mediated decay structure the biological variation. Long-read RNA sequencing directly observes full-length isoforms and alternative splicing graphs, at the cost of more complex cDNA synthesis artifacts and reverse transcription dropouts; direct RNA sequencing avoids reverse transcription but introduces motor-dependent dwell features that confound homopolymeric stretches. Single-cell protocols add a further sampling layer: molecular capture becomes a Bernoulli trial per molecule, leading to zero-inflated count distributions and requiring models that separate technical and biological zeros. Batch effects in droplet chemistry or cell lysis can outrun the biological signal unless addressed with explicit negative controls, spike-ins, and joint normalization-clustering approaches. On the other hand, full-length single-cell long-read protocols now reveal isoform switching across differentiation, altering the interpretation of bulk splicing kinetics in ways that are only now being formalized in models that integrate RNA velocity with structural isoform graphs. [8]

Epigenetic mapping illustrates the entanglement of signal and inference in an acute way. Sodium bisulfite treatment converts unmethylated cytosines to uracils, collapsing sequence complexity and creating asymmetries in mappability that complicate CpG island borders. Enzymatic alternatives preserve DNA integrity but introduce enzyme-specific biases whose calibration is nontrivial. Single-molecule approaches detect methylation either as kinetic perturbations in polymerase stepping or as shifts in nanopore current levels; both require training data that span sequence contexts and modification densities representative of the intended application space. The domain shift from cultured mammalian cells to plant genomes with 5mC in non-CpG contexts challenges models whose k-mer embeddings were learned on human libraries. Conceptual debates persist around 6mA in eukaryotesartifact or rare signaland around the appropriate hierarchical model linking methylation calls across reads to cell-type-level methylomes in heterogeneous tissues. Though co-profiling modalities that join chromatin accessibility, methylation, and transcript abundance in the same cell promise mechanistic insight, they multiply noise sources and impose joint priors that can be fragile when any one channel underperforms [9]. On the other hand, direct detection of nucleosome footprints and DNAprotein contacts from nanopore signal is opening an analysis space where the instrument measures biophysics more than sequence, and where inference architectures must be redesigned accordingly.

Operational economics transforms these technical considerations into study design. Throughput, expressed as bases per run, combines with run time to determine calendar-time latency; library prep complexity dictates labor cost and error rates; compute budgets for basecalling and alignment increasingly dominate total outlay as models become larger and more accurate. Storage is not incidental: raw signal files for single-molecule runs can exceed hundreds of gigabytes per flow cell, and lossy compression choices introduce subtle biases if downstream training uses compressed data. Multiplexing strategies balance per-sample cost against index misassignment; scheduling constraints in clinical settings disfavor oversized batches that delay answers. Quality control thresholdsQ30, N50, aligned-base fractionare proxies that must be tuned to the biological question, since maximizing them blindly can se-

lect against informative but difficult sequences such as GC-rich promoters or repetitive immune loci. Supply-chain fragility and lot-to-lot reagent variability are not footnotes; they are random effects that must appear in power calculations when timelines matter [10]. A seemingly unrelated systems constraintelectrical stability of the lab during monsoon seasonhas been known to dominate failure modes more than chemistry, a reminder that feasibility is an end-to-end property rather than a feature of a single box.

When platforms are treated as black boxes, investigators often misattribute failure modes to bioinformatics. That diagnosis reverses cause and effect. The mappability of an insertion flanked by low-complexity sequence is dictated as much by fragment size distribution and read length as by the choice of aligner index. Somatic variant detection at $<1\%$ variant allele frequency is constrained by pre-PCR damage, polymerase error profiles, and the availability of unique molecular identifiers that enable error suppression; calling is secondary to data generation in such regimes. Reference choice exerts its own leverage: graph-based references integrate alternate alleles and resolve pangenomic structure, raising sensitivity in ancestrally diverse cohorts while complicating downstream tools that assume linear coordinates. The ethical layer is not external either: adaptive sampling that depletes host DNA in real time can sharply improve infectious disease sensitivity, yet it raises questions about incidental findings if human reads are discarded before consent workflows apply. Though it is tempting to segregate chemistry from computation, maximal information is extracted only when these are co-designed and co-validated on representative specimens, with negative controls that interrogate each hypothesized failure mode rather than generic no-template blanks. [11]

Study design under constraints compels explicit trade-offs. For high-ploidy plant genomes with long, near-identical repeats, long-read sequencing with sufficient molecule length to bridge repeat units is not optional; localized polishing with short reads will not rescue assembly breaks where repeats exceed the longest molecules. Conversely, for large human cohorts studying common variant associations, short reads remain unmatched in cost efficiency and uniformity, provided that biases are modeled in the association test and that population structure is accommodated. Hybrid designsshort-read depth for power, long-read validation for structurecan work if the study allocates budget to a calibration subset in which both data types are collected to learn translation functions between them. Sample type matters in underappreciated ways: formalin-fixed, paraffin-embedded tissues carry damage signatures and fragmentation that push data generation into specialized pipelines with enzymatic damage correction and molecular indexing; fresh-frozen samples unlock different error models and longer molecules. A brief but instructive digression: freezethaw cycles alter chromatin accessibility in ATAC-seq more than they alter bulk RNA-seq, leading to uncorrelated QC flags across modalities that must be reconciled at the experimental design stage, otherwise cross-modality integration shifts from biology to artifacts without announcing itself.

Machine learning architectures sit at the heart of inference, but their behavior is bounded by the physics of the generating process [12]. Basecallers trained on curated ground truth can interpolate within the convex hull of observed contexts; extrapolation to novel k-mers or modifications depends on inductive biases built into convolutional receptive fields, attention mechanisms, or state-space models of signal drift. Alignment with learned seed scoring and adaptive banding exploits the same principle, converting algorithmic heuristics into differentiable components tuned from data. Yet model capacity is not a free lunch: larger models demand more compute and introduce stability issues when weights are pushed into regimes with sparse supervision. Synthetic spike-ins, calibration mixtures, and orthogonal truth sets (e.g., trio data with Mendelian consistency constraints) are not mere validation niceties but essential training signals that anchor learning in biology. A single contradiction will be tolerated by most downstream workflowsa well-calibrated caller might reduce precision to preserve recall in clinically actionable lociyet repeated contradictions signal that the assumed data-generating distribution has shifted, calling for retraining or re-instrumentation rather than parameter tweaking.

The fields most consequential tensions are now architectural. One camp argues for maximal unification: a pangenome graph reference, long reads for structure, short reads for cost, single-cell multiomics for mechanism, and end-to-end differentiable inference that ingests raw signals [13]. Another emphasizes modularity and interpretability: well-understood algorithms with explicit error models, separate data types for orthogonal views, and conservative integration strategies that make falsification straightforward. Both perspectives have merit. The unifying view promises acceleration and transfer learning across tasks; the modular view offers robustness and explainability in clinical contexts where failures must be understood before they are corrected. On the other hand, the decisive resource will likely be representative training data synthesized from diverse ancestry, tissue types, and environmental exposures, without which any architecture will overfit to the narrow slice of biology that is easiest to obtain. The communitys challenge is to build consortia, benchmarks, and governance models that keep pace with the devices themselves.

Recommendations framed in discipline-specific implications follow from this analysis. For assemblies of repeat-rich genomes, prioritize molecule length distributions that exceed the 99th percentile repeat unit; budget depth to guarantee at least 30Œ unique coverage after mappability masking; and include orthogonal long-range constraints so that mis-joins trigger conflicts rather than silent acceptance [14]. For tumor profiling where subclonal archi-

tecture is central, impose unique molecular identifiers at library inception, fit a site-specific error model that accounts for damage and context, and design cohorts with replicate biopsies that permit estimation of sampling variance across spatially distinct regions. For transcriptomics where isoform-specific regulation is plausible, collect a long-read calibration subset sufficient to train or select a bias-aware short-read quantifier, and validate claims on spike-in ground truth or synthetic constructs. A final operational note that rarely appears in methods sections: model the full pipeline as a queueing system with failure probabilities at each stage, since the highest scientific yield often comes not from marginally better chemistry but from reducing the variance of turnaround time that silently shapes which hypotheses can be tested in living projects.

Sequencing Platform Architectures and Reaction Kinetics

Contemporary sequencing technologies separate most cleanly along two orthogonal axes: the independence of per-symbol errors and the coherence length of molecular signal. Illuminas cyclic sequencing-by-synthesis represents the low-error, short-memory extreme. By engineering clonal ensembles that evolve in near lockstep, it generates base calls whose per-cycle error rates are low and largely uncorrelated, allowing simple depth accumulation to drive consensus accuracy into the Q30Q40 regime. The price is contiguity: molecules of a few hundred base pairs cannot span kilobase-scale repeats or phase long haplotype blocks, and the effective channel memory is bounded by insert size and paired-end geometry.

Pacific Biosciences single-molecule real-time system (SMRT) with circular consensus (HiFi) reads alters this geometry. Rather than collapsing information into short independent observations, it trades higher single-pass error for long correlated trajectories through templates that can exceed tens of kilobases. Consensus over repeated traversals reshapes the error spectrum from frequent stochastic miscalls into rarer, structured events [15]. The resulting channel retains long coherence while approaching substitution accuracy levels once thought exclusive to short reads, thereby unlocking assemblies and variant detection in regions where short-read depth cannot rescue structure.

Oxford Nanopore devices extend the coherence axis still further. A single molecule can be observed across hundreds of kilobases, sometimes spanning entire chromosomes or transcript isoforms. The electrical signal, however, is generated in a regime of overlapping k-mer states and stochastic motor stepping, yielding error distributions that are heavy-tailed and context-sensitive. Indels dominate, and substitution profiles vary with pore chemistry and electrolyte composition. From a channel perspective, nanopores deliver unprecedented context length at the expense of calibration stability: each pore and run drifts, demanding frequent retraining or adaptive decoding to sustain accuracy.

Against this backdrop, comparisons are more nuanced than short versus long reads [16]. Each architecture defines a different information channel with characteristic transfer functions, noise spectra, and calibration behaviors. Illumina offers depth-driven reliability for small variants across large cohorts; PacBio HiFi balances length and accuracy for assemblies and phasing; Nanopore delivers maximum contiguity and native modification detection at the cost of elevated raw error. Improvements in basecalling, consensus modeling, and quality recalibration continuously reshape the operating point of each system, narrowing gaps that once seemed structural.

When comparing modern sequencing technologies, Illumina remains the gold standard for short-read accuracy, while Oxford Nanopore provides ultra-long reads but with higher error rates. PacBio HiFi sequencing offers both long reads (10,000+ base pairs) and high accuracy, making it especially useful for genome assembly and variant detection. However, challenges remain in detecting somatic mutations with single-read quality scores. Recent work introducing TopoQual has addressed this issue by improving base quality predictions and correcting nearly one-third of sequencing errors in HiFi data [17].

The mechanistic origins of these differences become evident when one examines the chemistry and physics of each modality. Sequencing-by-synthesis (SBS) renders DNA into image sequences by orchestrating four constraints that rarely align perfectly: a polymerase must accept modified nucleotides with high fidelity; the reversible terminator must halt extension with near-unity efficiency; the fluorophore must emit enough photons before bleaching; and surface-tethered clusters must remain sufficiently synchronous that the aggregate signal per cycle retains discriminatory power.

Sequencing-by-synthesis (SBS) renders DNA into image sequences by orchestrating four constraints that rarely align perfectly: a polymerase must accept modified nucleotides with high fidelity; the reversible terminator must halt extension with near-unity efficiency; the fluorophore must emit enough photons before bleaching; and surface-tethered clusters must remain sufficiently synchronous that the aggregate signal per cycle retains discriminatory power.

Polymerases engineered for bulky dye–linker adducts face a kinetic trade: bulky groups slow catalysis and improve termination, smaller groups accelerate extension and leak phasing. The cleavage step restores the 3′-OH, yet incomplete deprotection produces “laggers” that dim the next frame; premature cleavage produces “leaders” that advance early. Either way, cluster coherence decays multiplicatively with cycle count.

Imaging systems respond by maximizing photon economy: high numerical aperture optics, TIRF illumination to reduce background, EMCCD or sCMOS sensors with calibrated gain, and spectral unmixing to control cross-talk among channels. Signal formation at the pixel level then obeys a variance budget—shot noise from finite photons,

Technology	Read Length	Error Rate	Coherence
Illumina (SBS)	100300 bp	∼0.1% (Q3040)	Short (insert size)
PacBio HiFi	1025 kb	∼1%	Long (repeated passes)
Oxford Nanopore	10 kb >100 kb	515%	Ultra-long

Table 1: Basic performance comparison of sequencing technologies.

Technology	Dominant Errors	Noise Spectrum	Calibration Needs
Illumina	Substitutions	Gaussian-like, cycle-dependent	Moderate (quality recalibration)
PacBio HiFi	Stochastic → structured	Semi-Markov kinetics	High (TopoQual, consensus)
Oxford Nanopore	Indels, context-sensitive subs	Heavy-tailed, 1/f noise	Very high (pore drift, retraining)

Table 2: Error and signal characteristics across platforms.

camera read noise, and spatial bleed—upon which phasing injects an additional, cycle-dependent broadening [18]. Paired-end chemistry recovers some lost information by interrogating the insert from both ends, provided the librarys size distribution is narrow enough that the two reads land in distinct genomic neighborhoods rather than chasing each other around adapters.

Control over cluster density sits awkwardly between chemistry and optics. Dense clusters raise throughput yet shrink inter-cluster distance, complicating deconvolution and increasing the risk of index misassignment via optical spill or template hopping during amplification. Temperature gradients across a flow cell alter polymerase kinetics and dye brightness, subtly warping quality score landscapes in a position-dependent manner. Base-specific error spectra reveal context coupling: homopolymers and GC-rich motifs yield asymmetric miscalls that recalibrators later treat as systematic. Quality scores, while nominally per-base probabilities, function in practice as sufficient statistics for many downstream filters because they encode cycle, context, and spatial covariates via the machine that trained them. A purely optical fix rarely suffices; the chemistry that reduces carry-forward also tends to diminish dye quantum yield, pulling SNR in the wrong direction [19]. However, depth rescues consensus so long as the error process remains stationary over the run and sufficiently independent across molecules.

Single-molecule real-time polymerase sequencing (SMRT) confines observation to zeptoliter volumes by embedding enzymes in zero-mode waveguides. Within that sub-diffraction cavity, binding events generate bursts whose intensity and duration report on base identity through a kinetic code: interpulse intervals (IPD) and pulse widths (PW) are distributed not as constants but as context-conditioned random variables. Dyelinker cleavage removes the fluorophore after incorporation, allowing continuous observation without cumulative crowding; the penalty is spectral overlap while multiple labeled nucleotides reside transiently in solution. Movie length becomes the experimental currency. Long films increase the chance that a single polymerase traverses large templates, while also courting photodamage and triplet-state blinking that complicate pulse detection. Circular consensus reads treat a hairpin-ligated template as a natural repetition code: the same insert passes repeatedly under observation, shrinking the posterior over the true sequence by repeated, conditionally independent looks that are not strictly independent because enzyme state drifts slowly [20]. Kinetic outliersextended IPDs at modified cytosines or adeninesenable detection of methylation without chemical conversion, a capability that depends on library integrity since nicked molecules induce pauses indistinguishable from modification signatures under naïve models.

A brief detour is warranted on instrumentation drift. Lasers age; alignment slips; dye lots vary in quantum yield; temperature and buffer composition wander across a long run. Laboratories that monitor reference constructs at fixed intervals discover low-frequency components in the time series of quality metrics that are invisible in per-movie summaries. Statistical process control, usually associated with manufacturing, becomes a sequencing tool here rather than an industrial curiosity, and not only for high-throughput cores.

Nanopore sequencing recasts the problem as electrical metrology. A pore constriction presents a set of conductance states indexed by the k-mer occupying the sensing region; a motor protein steps the nucleic acid so that the residence time of each k-mer matches the bandwidth of the amplifierADC chain [21]. The recorded trace is a superposition: deterministic shifts from mean k-mer conductance, thermally induced fluctuations, colored 1/f noise from electronics, and occasional spikes from transient pore interactions. Skip and stay events introduce misalignment between physical position and measured state count, so basecalling must operate on a latent segmentation that neither aligns perfectly with motor stepping nor with a fixed sampling grid. Early decoders imposed a hidden Markov model with Gaussian emissions and duration distributions, while contemporary approaches learn a direct mapping from raw current to sequence via convolutional or transformer encoders trained with CTC or transducer losses. The motor enzymes properties confine achievable accuracy: too fast and the states blur, too slow and practical throughput collapses. Pore engineeringmutations near

Application	Best Platform	Rationale	Limitations
Small variant detection (GWAS)	Illumina	High accuracy, depth-driven	Poor contiguity
Genome assembly & phasing	PacBio HiFi	Long, accurate reads	Cost, somatic mutation calls
Epigenetics / RNA isoforms	Nanopore	Native signal, ultra-long reads	Elevated raw error

Table 3: Optimal platform selection by scientific objective.

the constriction, alternative scaffolds such as CsgG derivatives, chemical modifications to the rimreshapes the discriminability landscape, changing not only per-base error but the effective alphabet. Direct RNA sequencing introduces base-specific and modification-specific perturbations to both dwell and current amplitude, simultaneously enriching signal and complicating models because folding intermediates act as kinetic branches that the motor occasionally resolves only after stochastic dwell.

An apparently peripheral variable manages to dominate real datasets: electrolyte composition and viscosity [22]. The ionic strength sets both the open pore current and the sensitivity per k-mer, while viscosity and temperature jointly fix diffusion coefficients that control noise bandwidth. Changing buffer for a new modification assay therefore alters baseline statistics for the unmodified case, confounding model transfer unless the training regime spans the operational space rather than a single optimal recipe that rarely survives contact with a new organism.

A unified modeling frame treats all three modalities as channels with distinct transfer functions mapping latent sequences to emissions. SBS yields per-cycle intensity vectors whose distributions approximate Gaussians with means determined by the base and variances that grow with cycle count and local dephasing; prephasing and phasing contribute off-diagonal terms if one writes the process in a linear state-space form. SMRT and nanopore generate single-molecule time series with memory: semi-Markov structure captures variable dwell times; context length exceeds one base because the sensing region covers multiple nucleotides; slow drifts introduce nonstationarity at minutes-long scales. Decoders built on these assumptions differ in architecture yet share an aimto invert the channel while quantifying uncertainty so that downstream inference can weight evidence sensibly. Learned basecallers estimate per-base posterior probabilities, not hard labels, and side channels such as kinetic features (SMRT) or raw current summary statistics (nanopore) become inputs to methylation callers that share the feature extractor while training separate heads. [23]

Training data define the ceiling. Synthetic constructs with known truth, microbial standards with high-quality references, and human trio samples that enforce Mendelian consistency provide complementary supervision. Distribution shift appears in two guises: new pore chemistries or polymerases change transfer functions; new genomes change k-mer frequencies and motif contexts that drive error asymmetries. Domain adaptation strategiesfine-tuning with small calibration sets, mixture-of-experts models that select sub-networks per chemistry, or self-training on consensus assembliespartially mitigate the shift while adding operational complexity that must be budgeted. A practical implication follows for study design: allocate sequenceable control material to every batch and run a standardized calibration protocol that yields a comparable likelihood scale across time, because downstream variant callers silently assume such comparability when they aggregate evidence across lanes or flow cells.

Information-theoretic intuitions sharpen the trade-offs that practitioners already exploit. SBS operates in a regime of low per-symbol error and short memory, so redundancy accrues through depth and through paired-end constraints that approximate parity checks across the insert; indel errors are rare and substitution-biased, aligning neatly with graph mappers optimized for seeds and extensions [24]. SMRT and nanopore function with higher symbol error yet long coherence length: redundancy accrues through coverage over long molecules, and the costs concentrate in segmental mis-joins rather than per-base noise once consensus is computed. The right abstraction is channel coding shaped by chemistry: circular consensus transforms a single-molecule channel into multiple uses of a nearly stationary subchannel; adaptive pore control shifts dwell-time distributions toward regimes with lower overlap of state distributions. However, no abstraction removes the entanglement with sample preparation, since fragmentation, nicking, and chemical damage sculpt the molecule population presented to any instrument in ways that the decoder can only treat as prior information rather than evidence.

Epigenetic readouts complicate the notion of ground truth. In SBS, bisulfite conversion or enzymatic alternatives confound sequence and methylation, forcing decoders to operate on an altered alphabet with asymmetric mappability. In SMRT and nanopore, modification is an effect on kinetics or current, not a base substitution, so joint calling must disentangle two latent variables per position: identity and mark. Semi-supervised training with sparse orthogonal labelsmass spectrometry validation, restriction enzyme sensitivityprovides anchors, yet cell-type heterogeneity means that the same locus exhibits mixtures of methylation states across molecules, inviting hierarchical models that pool across reads while preserving per-molecule evidence. Debates persist over optimal parameterization: should one attach modification probabilities to bases during basecalling, or stage the problem and call modifications on stabilized alignments to the reference or to a local assembly. [25]

Operationally, the implications are precise. If the sci-

entific objective hinges on small substitutions in large cohorts, SBS with rigorously controlled insert sizes and calibrated quality models delivers the most stable likelihoods for association tests. If the goal is to resolve structural repeats or phased haplotypes across tens of kilobases, SMRT and nanopore provide the necessary context length, on the condition that processivity and motor stepping are tuned to avoid segmentation collapse in low-complexity regions. For projects prioritizing methylomes or direct RNA, plan for chemistry-specific training and validation, since transfer from DNA models rarely achieves clinical-grade calibration. Final caution, not as an afterthought: laboratories that treat these platforms as interchangeable black boxes absorb unmodeled variance into bioinformatics, when the variance originated upstream in the channels transfer function and its drift over time, an allocation error that repeats itself even in well-resourced settings.

Library Preparation, Molecular Tagging, and Read Length Distributions

Decisions at the library step define the distributions of fragment length, end repair fidelity, and molecular identity tracking that govern effective coverage and bias. Mechanical shearing combined with end repair and adapter ligation creates a broad fragment spectrum, typically approximated by a log-normal distribution whose parameters depend on input mass and shearing energy [26]. Size selection by beads or electrophoresis truncates tails and sharpens modal length, directly affecting mappability across repeats and GC-rich segments. For short-read platforms, paired-end libraries with a defined insert distance allow recovery of adjacency information spanning low-complexity regions whose individual reads lack unique anchors. For long-read platforms, high-molecular-weight extraction and gentle handling aim to maintain tens to hundreds of kilobases, while transposase-based rapid protocols trade maximal length for simplicity and speed.

Unique molecular identifiers introduced prior to amplification label original molecules and decouple PCR duplication from true coverage. Under UMI usage, consensus reads per molecule approach the amplification error floor, enabling precise variant detection in low-allele-fraction contexts. Barcode collision rates follow occupancy statistics that depend on barcode space size and the number of molecules; increasing the diversity of the tag space reduces collisions but expands index bleed-through risks if sequencer crosstalk is poorly calibrated. For single-cell assays, combinatorial indexing or droplet microfluidics couples cell barcodes and UMIs to transcript fragments, with collisions manifesting as doublets that can be computationally identified by genotype or expression outliers when background rates and barcode distributions are modeled.

Targeted capture and amplicon strategies reshape the coverage distribution relative to whole-genome shotgun sampling [27]. Hybrid-capture with biotinylated baits introduces sequence-specific hybridization kinetics that vary with GC content and secondary structure, producing systematic underrepresentation of extreme-content regions unless bait design compensates with density and melting temperature adjustments. Amplicon panels impose tiled PCR constraints, with primertemplate mismatches degrading efficiency and preferentially dropping out variant alleles near primer sites. Long-amplicon designs for third-generation instruments face polymerase stall risks at structured or damaged sites, skewing read length and complicating consensus if coverage is uneven.

A practical modeling approach specifies the library as a mixture distribution over fragment lengths and molecular classes, then propagates this mixture through platform-dependent read generation. For a given genome of length G, fragment count N_f with length distribution $p_L(\ell)$, and platform-specific readout function $r(\ell)$ giving expected usable bases per fragment, the expected nominal coverage becomes $c = \frac{N_f \, \mathbb{E}[r(L)]}{G}$. Deviations from nominal arise from mappability constraints, duplication, and capture bias that can be estimated by fitting negative binomial models to observed depth histograms with covariates for GC, mappability, and bait density. This statistical lens provides levers to redesign libraries and balance trade-offs between insert length, UMI density, and protocol complexity.

Signal Generation, Basecalling, and Error Modeling Across Platforms

Continuous improvements in basecalling reflect a shift from hand-crafted signal features to deep sequence models that learn effective representations from raw time series or images [28]. Sequencing-by-synthesis historically used per-cycle intensity normalization and phasing correction, then called bases via deconvolution and probabilistic calibration of quality scores. The residual error spectrum shows context-linked substitutions and indels clustered near homopolymers when dephasing and saturation degrade signal separation. Single-molecule polymerase movies generate multi-channel temporal streams where pulses arise from bound nucleotides, with inter-pulse durations and widths providing orthogonal cues. Modern decoders ingest these pulse trains with recurrent or attention architectures that can output both base sequences and modification likelihoods by conditioning on kinetic features.

Nanopore basecalling involves segmentation of current traces into events and mapping those events to k-mer labels via hidden Markov models or, increasingly, neural connectionist temporal classification and transducer frameworks. Let $x_{1:T}$ denote the sampled current, and $y_{1:K}$ the latent base string. A generic probabilistic decoder maximizes a regularized log-likelihood

$$\mathcal{L}(\theta) = \log \sum_{a \in \mathcal{A}(y)} p_\theta(a \mid x_{1:T}),$$

where a ranges over alignments in a monotonic alignment lattice that permits stays, skips, and insertions [29]. Parameter vector θ describes convolutional front-ends that

Platform	Fragment Handling	Typical Lengths	Constraints
Illumina (short-read)	Mechanical shearing + ligation	200–600 bp inserts	Log-normal; size-selected
Long-read (PacBio, ONT)	HMW extraction, gentle prep	10 kb – >100 kb	Shear-sensitive
Rapid protocols	Transposase tagmentation	1–10 kb	Shorter, faster

Table 4: Fragment and read length distributions by platform.

Tagging Strategy	Function	Advantages	Limitations
UMIs	Track original molecules	Reduce PCR artifacts; variant calling	Barcode collisions
Cell barcodes (single-cell)	Assign reads to cells	Enables single-cell resolution	Doublets, background noise
Combinatorial indexing	Expand barcode space	High multiplexing	Crosstalk, collision risk

Table 5: Molecular tagging approaches and trade-offs.

capture local motifs and recurrent or transformer layers that model long-range dependencies induced by pore context memory. Calibration with control DNA yields mappings from raw logits to calibrated quality values $Q = -10 \log_{10} p_e$, but miscalibration can occur when sample composition diverges from training priors, a concern in metagenomes or modified bases not present during training.

Error modeling benefits from decomposing errors into independent and correlated components. For short-read cyclic methods, per-cycle phasing introduces correlated substitution patterns manifested as systematic undercalls or overcalls of homopolymers, well captured by autoregressive error terms that grow with cycle number. For single-molecule modalities, indels dominate due to event segmentation ambiguity or polymerase pausing, with context-dependent dwell-time distributions leading to asymmetric insertion and deletion rates near repeats. A semi-Markov framework with state-specific duration distributions $p(d \mid s)$ provides a realistic generative account of event lengths, and Viterbi or beam-search decoders constrained by these durations reduce indel bursts without sacrificing speed.

Consensus algorithms transform raw read errors into highly accurate assemblies or haplotype-resolved contigs by integrating overlapping evidence. Under a simplified independent error model with per-base error rate ϵ and m concordant reads, the probability that majority vote yields a wrong consensus at a locus can be bounded using Chernoff inequalities [30]. For odd m, a direct expression for the probability of an incorrect majority is

$$P_{\text{err}} \leq \sum_{k=\lceil m/2 \rceil}^{m} \binom{m}{k} \epsilon^k (1-\epsilon)^{m-k}.$$

Although independence is violated by context-correlated errors, empirical reduction of errors from ten percent to below one in ten thousand through multi-pass circular consensus or pileup-trained neural correctors demonstrates the effectiveness of redundancy. Hybrid polishers that align short reads to long-read assemblies exploit complementary error spectra: systematic indels in long reads are corrected by precise short-read anchors, while long read context disambiguates repetitive placements that confound short-read-only polishing in low-mappability regions.

De novo Assembly, Variant Detection, and Haplotype Resolution

Contig construction from reads derives from graph-theoretic representations whose structure reflects platform properties. Short-read assemblers favor de Bruijn graphs with k-mer nodes, reducing memory demands and accommodating astronomical read counts, but fragment repeats longer than k introduce bubbles and tangles that require paired-end or long-insert mate-pair edges to resolve. Long-read assemblers often operate on overlap graphs where edges represent alignments between reads; minimizer-based sketches reduce computational burden by hashing sparsified k-mer subsets that preserve locality while discarding noise. Error rates in long reads mandate sensitive overlap detection followed by aggressive consensus, yet the increased scope across repeats transforms repeats into traversable segments, collapsing graph complexity. [31]

Coverage theory connects fragment sampling to gap probability and contiguity. Under the LanderWaterman model with mean coverage c, the probability a base remains uncovered is approximately e^{-c}, while the expected number of contigs under idealized conditions scales with $G\, e^{-c}/\mathbb{E}[L]$ for mean read length $\mathbb{E}[L]$. These expressions neglect mappability and structural biases; nonetheless, they illuminate why long-read lengthening yields superlinear gains in N50 when encountering repeats. Adding accurate long-range linking such as Hi-C or optical maps supplies orthogonal constraints that lift residual ambiguities in segment orientations and scaffolding. Phasing extends assembly by assigning variants to haplotypes using read co-occurrence patterns across heterozygous sites. In diploid human genomes, long reads spanning multiple heterozygous sites directly support phasing blocks that approach chromosomal scale, while statistical phasing using reference panels fills gaps in low heterozygosity regions at the cost of population-dependent assumptions.

Variant detection stratifies into single-nucleotide variants, small indels, and structural variants. Short reads

Strategy	Mechanism	Bias Sources	Notes
Whole-genome shotgun	Random shearing	GC/mappability bias	Broadest coverage
Hybrid capture	Biotinylated baits	GC, structure, melting temp	Design-dependent
Amplicon panels	PCR tiling	Primer mismatches, dropout	Allele bias near primers
Long-amplicon (3G)	Polymerase traversal	Stall at damage/structure	Uneven coverage

Table 6: Targeted vs. genome-wide library strategies.

excel at SNVs and small indels in regions with unique mapping; probabilistic callers integrate base qualities, mapping qualities, and local haplotype likelihoods to assess evidence under diploid or somatic models [32]. Indel detection degrades as indel length approaches read length or spans microhomologies that induce alignment ambiguity. Long reads shift the sensitivity frontier for structural variants, capturing insertion sequences, complex breakpoints, tandem repeat expansions, and mobile element insertions in a single read or a small pileup. Breakpoint precision depends on alignment heuristics sensitive to high-error reads; graph-aware mappers that internalize alternate alleles as parallel paths avoid reference bias and improve breakpoint localization.

Somatic variant calling in tumors adds subclonal mixtures, copy-number changes, and aneuploidy that distort allele fractions. Depth from short reads provides statistical power for low-frequency variants, but context complexity and copy-numberaware priors become essential to avoid artifacts. Long reads contribute disambiguation across paralogous genes and repetitive promoters where short-read mappability falters, and they enable phasing of somatic variants with germline backgrounds to reconstruct clonal architecture. For highly rearranged cancer genomes, assembly-first strategies using long reads reconstruct event graphs that allow cleaner identification of templated insertions and chromothripsis patterns that evade short-read local callers. [33]

Multi-omic Profiling with Sequencing: Epigenomes, Transcriptomes, and Spatial Context

Native chemical information carried by nucleic acids provides an extended alphabet that sequencing can capture when the transduction physics remains sensitive to base modifications. Polymerase kinetics deviate upon encountering methylated cytosines or other modifications, creating characteristic dwell-time signatures; nanopore currents shift in a modification-specific manner due to altered base-pore interactions. When basecalling models are trained to output modification probabilities conditioned on raw signals, methylomes and other modification maps become first-class outputs rather than derived tracks. Unlike bisulfite conversion, which reduces alphabet size and introduces conversion inefficiencies tied to sequence context, direct detection retains base identity and leverages co-occurrence patterns of modifications across long stretches to detect allele-specific methylation and phase-dependent regulatory states.

Transcriptomics benefits from both depth and contiguity. Short-read RNA sequencing quantifies transcripts by counting exonic reads and inferring junction usage via splice-aware alignment, yet remains susceptible to isoform ambiguity in gene families with shared exons. Long-read cDNA and direct RNA protocols produce full-length isoforms that pass through complex splice junction chains, exposing exon skipping, intron retention, and alternative polyadenylation without assembly [34]. Direct RNA sequencing additionally preserves native poly(A) tail lengths and internal modifications such as m6A, broadening the accessible transcript features. Error rates in long-read RNA data complicate quantification at low expression, but transcript-level priors and expectationmaximization over read-to-isoform assignment stabilize estimates, especially when reference transcriptomes provide structural constraints.

Spatial assays couple molecular barcodes with physical coordinates in tissue. One class of methods captures transcripts onto spatially barcoded arrays followed by short-read sequencing, thereby conferring positional information but truncating contiguity. Emerging integrations combine long-read capture with spatial indexing, which promises isoform-resolved spatial expression maps, though reduced per-spot molecule counts impose statistical challenges. Multi-omic single-cell platforms that jointly assay chromatin accessibility and gene expression share barcodes across modalities, enabling direct coupling of regulatory state and transcriptional output. Long-read information can reveal allele-specific chromatin states and repetitive element activity, enriching models of regulatory grammar that are otherwise incomplete under short-fragment observations. [35]

Metagenomics illustrates a distinct advantage of long reads where strain-level resolution hinges on crossing repeated operons and mobile elements. Short reads fragment assemblies across ribosomal operons and repetitive islands, blurring boundaries between strains in complex communities. Long reads that span operons and flanking unique regions yield contiguous bins with resolved plasmids and integrated phages. Direct detection of DNA modifications across microbes contributes to hostphage interaction inference, as restrictionmodification patterns and methylation motifs act as molecular fingerprints of lineage and ecological interaction.

Throughput, Cost Models, and Design Optimization for Genomic Studies

Instrument selection intertwines with throughput constraints and cost minimization under accuracy targets. A useful abstraction treats a sequencer as a production line whose yield depends on occupancy, per-channel output, runtime, and usable fraction after quality filters. Let F denote the number of active features (clusters, zero-mode waveguides, pores), b the average bases per feature per unit time, η the fraction of time features produce signal, and T the run time [36]. Expected raw yield is $Y_{\text{raw}} = F\,b\,\eta\,T$. Usable yield multiplies this by quality acceptance q and mapping fraction m, yielding $Y_{\text{use}} = Y_{\text{raw}}\,q\,m$. For nanopores, F varies over time as pores die or recover; a simple model uses a birthdeath process with rates λ and μ, giving expected active pores $E[F(t)] = F_0 e^{-(\mu-\lambda)t} + \lambda F_0(1-e^{-(\mu-\lambda)t})/(\mu-\lambda)$ when $\mu \neq \lambda$. Integrating $E[F(t)]$ across T captures decaying throughput and motivates adaptive scheduling of reloads.

Per-sample cost decomposes into fixed and variable components. If C_{run} is the consumable and amortized instrument cost per run and n samples share the run, the per-sample fixed cost is $C_{\text{fix}} = C_{\text{run}}/n$. Variable cost scales with target coverage and library complexity: $C_{\text{var}} = \alpha\,c\,G$ where α captures reagent cost per base and cG is the target number of mapped bases. Total cost $C = C_{\text{fix}} + C_{\text{var}} + C_{\text{lib}}$ includes library preparation cost C_{lib} that may dominate for low-input or single-cell assays. Optimization sets c to meet accuracy constraints. For variant detection with majority consensus, one can target a posterior error rate δ at heterozygous sites by solving for c such that the probability of incorrect consensus under an effective per-read error ϵ falls below δ. Under a binomial approximation, a conservative choice satisfies

$$\sum_{k=\lceil m/2 \rceil}^{m} \binom{m}{k} \epsilon^k (1-\epsilon)^{m-k} \le \delta,$$

with $m \approx c$ when coverage equals read count per locus. In practice, overdispersion and context correlation inflate required coverage relative to the ideal independent model; introducing a dispersion factor ϕ via a betabinomial correction increases the tail probability and yields larger c for the same δ. [37]

Study design faces a fundamental trade-off between depth per sample and number of samples. For discovery of rare variants with population frequency f, the power to observe at least r carriers increases with cohort size N as $1 - \sum_{k=0}^{r-1} \binom{2N}{k} f^k (1-f)^{2N-k}$, assuming diploidy and independence. If per-sample cost scales linearly with coverage, budget-constrained optimization under a fixed total cost B allocates $N = \lfloor B/C(c) \rfloor$ and chooses c to meet per-sample calling accuracy. This decoupling breaks when sample preparation imposes minimum lot sizes or when batch effects raise the effective error rate ϵ unless depth compensates. For long-read assemblies, increasing per-sample coverage above approximately thirtyfold often transitions contiguity from fragmented to near-complete for human genomes, but gains saturate beyond fiftyfold absent extreme repeats or polyploidy. Short-read resequencing for small variant discovery typically stabilizes beyond thirtyfold as well, provided mappability and GC bias are controlled; exomes require different scaling because capture inefficiencies alter the effective coverage distribution across targets.

Turnaround time models reflect serial and parallelizable components. Library preparation and size selection contain hands-on steps that can be parallelized across samples, whereas run time is largely instrument-bound [38]. For clinical settings, constraints on maximum time to result push designs toward protocols with minimal incubation and straightforward QC checkpoints. Long-read workflows that avoid PCR and preserve modifications shorten hands-on time but may require higher input mass; short-read workflows can be miniaturized and automated to reduce operator variability at the expense of added QC steps for capture uniformity.

Quality Assurance, Standards, and Interoperability in Sequencing Workflows

Reproducibility in sequencing arises from consistent laboratory procedures, validated computational pipelines, and reference materials that anchor performance. Without explicit standards, comparisons across instruments or across releases of chemistry and basecallers conflate biological differences with process changes. Quantitative process control tracks distributions of key metrics such as insert size, duplication rate, per-cycle error, and phasing parameters for cyclic chemistries, or pore occupancy, event rate, and dwell-time quantiles for nanopores. Control charts with pre-specified alarm thresholds detect drift; when control DNA is run alongside samples, deviations in calibrated quality distributions immediately reveal detector or chemistry issues.

Cross-platform interoperability depends on common exchange formats that retain raw signal and metadata [39]. While aligned reads provide convenience, access to raw signals enables reprocessing under improved models and supports secondary analyses such as modification detection not envisioned during initial sequencing. Quality value calibration must be consistent to avoid misinterpretation by downstream variant callers that rely on log-odds semantics. If recalibration adjusts quality distributions, downstream tools must be informed through updated headers to maintain probabilistic coherence.

Benchmarking practices require careful construction of truth sets that cover diverse genomic contexts. Truth sets limited to easy regions inflate apparent performance and mislead deployment decisions in clinical pipelines. Including challenging regions such as segmental duplications, tandem repeats, and GC extremes exposes error modes and guides targeted protocol improvements. Long-read

truth construction itself relies on assemblies and orthogonal evidence, and must be updated as assembly algorithms and polishers improve; frozen truth sets risk fossilizing outdated biases [40]. For transcriptomics, truth manifests as spike-in controls and synthetic constructs that probe isoform boundary detection and poly(A) tail estimation, yet biological diversity quickly exceeds the scope of spikes, reinforcing the need for transparent uncertainty reporting in quantification outputs.

Batch effects remain a persistent concern. Index hopping, barcode cross-talk, and reagent lot differences generate systematic artifacts that mimic biological signals. Balanced experimental designs with randomized samples across lanes, flowcells, and reagent lots mitigate confounding. Statistical models that absorb batch factors and exploit technical replicates reduce spurious discoveries, but they cannot rescue designs where batch is aliased with biological groups. For long-read epigenetic detection, drift in pore chemistry or motor proteins shifts current distributions, necessitating periodic retraining or transfer learning to maintain calibration across batches.

Ethical, Regulatory, and Clinical Translation Considerations for Platform Choice

Clinical deployment imposes constraints beyond raw performance, including validation requirements, data retention policies, patient privacy, and interpretability of results [41]. Instruments and assays must pass analytical validation demonstrating accuracy, precision, reportable range, and limits of detection under intended-use populations and specimen types. Short-read platforms with long-standing regulatory familiarity offer a smoother validation path for small-variant assays in well-characterized genes, while third-generation systems enable assays that cannot be equivalently implemented with short fragments, such as repeat expansion sizing, complex structural variant detection, and methylation-informed classification. Validation strategies must align performance claims to clinical questions; for example, a long-read assay targeting repeat expansions should specify validated size ranges, mosaic fraction sensitivity, and inter-laboratory concordance.

Data governance weighs storage of raw signals against reanalysis benefits. Retaining raw movies or current traces facilitates future reinterpretation as decoding models mature, yet increases storage footprints and raises privacy concerns if raw signals inadvertently reveal sample-specific signatures beyond sequence. Compression with lossy schemes tailored to signal characteristics may preserve downstream utility while reducing burden, but clinical policies must define acceptable distortion and document its impact on analytical validity. Turnaround time and chain-of-custody protocols require harmonization with laboratory information systems, including deterministic sample tracking across multiplexed runs and explicit audit trails for demultiplexing and basecalling versions. [42]

Equity considerations emerge in population sequencing and newborn screening. Platform choice influences the spectrum of detectable variation; reliance on short reads may underrepresent structural variation enrichments found in under-studied populations, while long-read cost and throughput constraints can limit inclusion if budgets are fixed. Hybrid designs offer a path to equitable representation by layering long-read sequencing on a subset of participants to build comprehensive references and training data that improve short-read inference in the broader cohort. Transparent communication of residual uncertainties in variant interpretation, especially in repetitive or GC-extreme regions, supports informed clinical decision-making and avoids overconfidence fueled by high nominal coverage.

Conclusion

Casting sequencing instruments as noisy channels clarifies both their capabilities and their failure modes. A latent genomic string passes through a transduction pipeline that imposes chemistry-specific distortions; a decoder then proposes hypotheses under priors and loss functions aligned to the studys aims. Treating the instrument as a channel with a transfer function makes concrete what platform choice actually means: one chooses error spectra, memory length, observable side channels, and throughput constraints, then chooses an inference strategy that converts emissions into calls with quantified uncertainty [43]. From this stance, small-variant association studies privilege channels with low independent per-base error, while structural genomics privileges channels with long coherence and informative side signals; however, both require explicit accounting for where evidence concentrates and where it thins.

Short-read cyclic chemistries implement a near-memoryless channel at the base level. Reversible terminators synchronize clonal clusters, imaging aggregates photons into four-color intensity vectors, and learned calibration translates those vectors to quality scores. Substitution errors dominate, indels are rare, and cycle-correlated phasing gradually widens the emission distributions. Because the channels memory is short and the per-symbol error is low, redundancy achieved through depth collapses uncertainty efficiently, making these systems natural fits for large cohorts and for applications where deep multiplexing and tight per-sample cost ceilings govern feasibility. The limits appear when the biological message depends on long-range linkagemulti-kilobase haplotypes, repeat-spanning arrangements, paralog disambiguationsince a short-memory channel cannot carry constraints beyond the insert and its paired-end echo. A laboratory can compensate with mate-pair scaffolds, linked fragments, or capture approaches, yet the compensation works only when library physics cooperate rather than fight the underlying channel. [44]

Single-molecule modalities invert the trade. Long molecules and native chemical sensing introduce a channel

with long memory and auxiliary observables: kinetic pauses and pulse widths in real-time polymerase systems; ionic current levels and dwell times in nanopore devices. The raw per-symbol error is higher, but evidence aggregates across correlated segments, and consensus modeling acts as error shaping rather than simple averaging. Context reach allows direct observation of structural variants, repeat traversals, and phase blocks that collapse neatly into biological statements. On the other hand, heavy-tailed error modesstalls, chimeras, skipstay dynamicsviolate Gaussian assumptions that underpin many textbook estimators, so decoders carry more modeling responsibility than in short-read pipelines. Native detection of modified bases adds a second latent variable per locus, converting basecalling into multi-task inference with competing objectives.

Application decisions, to be defensible, should be phrased as interactions between error spectra and biological structure [45]. Tandem arrays punish channels that confuse homopolymers; mobile elements punish channels that cannot bridge long identical copies; paralogs punish channels that collapse reads onto the wrong locus unless k-mer uniqueness is preserved. Allele-specific regulation requires phase-aware quantification or signal averages blur cis and trans effects; splicing complexity requires fragment models that admit multiple paths through an isoform graph rather than a single dominant transcript. A design that reads as long reads for repeats, short reads for depth becomes actionable only when translated into thresholds: repeat unit lengths versus molecule N50, paralog divergence versus k-mer size, splice graph edge count versus fragment-length prior. A digression is warranted: freezer dwell time before plasma separation alters cell-free fragmentomes sufficiently to shift tumor fraction estimates, which means that channel selection without sample-handling priors risks confounding that no decoder can repair.

Equations supply the grammar for these translations. Start with coverage: under idealized Poisson fragmentation, the expected uncovered fraction is e^{-C}, yet real fragmentation and mappability alter the effective depth to $C_{\text{eff}} = C \cdot \alpha \cdot m$, where α captures duplication and bias, and m masks unmappable bases. For assemblies, the probability of bridging a repeat of length R with molecules distributed as $L \sim f(L)$ at per-base coverage C is $1-\prod_L [1-C\cdot \Pr(L>R)]$, which sets contiguity limits independent of nominal read length statistics. Phasing block length scales with the rate of heterozygous markers θ, switch error s, and molecule span, leading to a rough expectation $E[\text{block}] \approx \frac{1}{\theta s}$ once long-range support decays, an expression that foregrounds caller calibration as much as data generation. In single-molecule channels, occupancy dynamics matter: let ρ denote active pores or wells, λ the productive rate per site, and τ the mean read duration; throughput follows $\rho\lambda\tau$, yet quality drifts if λ is raised via motor speed beyond the segmentation bandwidth. [46]

Loss functions complete the framing. A clinical screen minimizes false negatives for actionable loci and tolerates confirmatory reflex testing; a population genetics study minimizes systematic bias across ancestry groups even if absolute error at a few loci rises; a de novo assembly prioritizes mis-join avoidance over isolated base errors. Formally, define a loss L over genotypes or contigs, not over bases, and tune decoders to minimize $E[L]$ under priors that reflect sample type and cohort composition. With explicit L, disagreements across platforms are not annoyances but instruments: divergent calls identify regions where the marginal contribution of long-range context exceeds its incremental error burden.

Budget allocation benefits from explicit trade curves. Let B be the total spend per cohort, p the per-sample library cost, s the per-sample sequencing cost, and $g(C)$ the marginal reduction in variant-calling loss with coverage C.

The optimal coverage C^* solves

$$g'(C^*) = \lambda,$$

where λ is the Lagrange multiplier induced by $\frac{B}{p+sC}$ and the desired cohort size.

In mixed designs, allocate a fraction β of samples to long reads with depth C_L and $1-\beta$ to short reads with depth C_S, selecting (β, C_L, C_S) to minimize the combined loss under a fusion model that maps long-read consensus to features usable by short-read callers and vice versa [47].

Library strategies that preserve molecular identitysuch as unique molecular identifiers (UMIs) and long inserts with controlled size distributionspush the trade curves favorably by converting raw depth into effective independent observations with known duplication structure.

Quality thresholds demand probabilistic coherence. A base quality score calibrated on one instrument chemistry cannot be used as-is in a joint caller trained on another without re-scaling, or the combined likelihoods become incoherent. The discipline here is to anchor quality to external truthmicrobial standards, trio consistency, spike-insthen use monotone transforms to place all evidentiary streams on a shared scale. Calibrated posteriors enable downstream tools to operate with Bayes-optimal thresholds rather than hand-tuned filters that drift across batches. Batch-aware priors belong in the model as formal parameters, not as tacit laboratory lore.

Hybrid pipelines succeed when integration respects each channels geometry [48]. Short reads supply dense, low-variance evidence for single-nucleotide variation and for polishing; long reads supply sparse, high-leverage evidence that resolves structure and phase. Graph-based references-pangenomes that embed alternative haplotypesprevent long reads from being forced through linear coordinates that fracture signals at structural breakpoints. Assembly-first workflows can pass polished contigs to short-read mappers for local error correction, while alignment-first workflows can promote ambiguous regions to local assembly, with arbitration by a reconciler that tracks provenance so

that later reanalysis can revisit marginal calls. Reference bias intrudes whenever a decoders search space is pruned by an assumed coordinate system; neutralizing that bias requires either symmetric representations or explicit penalization of alignment overfitting, a point that often surfaces only during replication studies.

Algorithmic interpretability sets the rate at which chemical or electronic improvements translate into durable gains. A larger basecaller raises accuracy on benchmarks today, yet deployment stalls if the models failure modes remain opaque to validation teams charged with clinical governance. Salient-feature attribution for raw signal segments, calibration curves stratified by sequence context, and counterfactual tests with synthetic constructs become part of the release checklist [49]. Standardization of file formats for raw emissions, intermediate features, and final calls allows cross-lab reproducibility and retrospective harmonization when decoders are upgraded; a laboratory that stores only basecalls forfeits the ability to reanalyze modified-base evidence when models improve next year, an avoidable loss.

Interpretability also threads through debates about end-to-end versus modular inference. One school argues for decoders that ingest raw signals and emit genotypes in a single differentiable graph trained on comprehensive labels; the gains in joint optimization and error propagation can be striking. A rival view keeps basecalling, alignment, and variant calling separate with explicit, exchangeable models, accepting occasional suboptimality in exchange for testability and clinical auditability. Neither camp wins universally. In discovery settings with rich training labels and homogeneous chemistries, end-to-end can dominate; in regulated pipelines where changes must be localized and justified, modularity often prevails. Yet both approaches founder without representative training distributions that include ancestrally diverse genomes, sample types with realistic damage profiles, and edge-case structures such as complex inversions near centromeres. [50]

Operational economics intrude at every decision node. Throughput measured as bases per day matters less if compute budgets for basecalling and alignment throttle delivery; cloud acceleration and on-instrument ASICs change the calculus by moving the bottleneck. Storage costs scale superlinearly when raw traces are retained; lossy compression must be documented and validated for downstream neutrality, not assumed harmless. Multiplexing improves per-sample cost until index misassignment converts rare-event detection into a false discovery factory; mitigation through unique dual indices and enzymatic cleanup carries its own price and failure modes. Experienced cores track energy stability and HVAC performance as carefully as reagent inventories; a run lost to a voltage sag costs more than incremental accuracy gains expected from a new basecaller revision.

Risk management for clinical or high-stakes studies suggests explicit contingency design. A planned long-read phase may slip due to pore supply; a fallback short-read depth must be precomputed to maintain sensitivity for the endpoints that cannot be deferred [51]. Confirmation pathwaysorthogonal assays for variants above a clinical actionability thresholdare specified in advance with triggers derived from posterior probabilities, not ad hoc read-depth heuristics. Audit trails that preserve random seeds, software versions, and parameter hashes keep disputes resolvable months later when an outlier result challenges a therapeutic decision. Laboratories that ritualize such planning discover that scientific agility increases, paradoxically, because the cost of changing course midstream declines.

Heterogeneous genomes and assays reward hybridization beyond simple two-platform blends. Proximity ligation (Hi-C) or Strand-seq adds directional constraints that excise mis-joins in repeats; synthetic long reads or barcoded partitioning reconstruct haplotypes without full single-molecule runs; targeted enrichment tilts coverage toward loci of mechanistic interest where long reads would otherwise be squandered across uninformative deserts. The joint prior linking these signals should be made explicit: a scaffold that expects fewer than k cut points per megabase; a haplotype block model with recombination-aware transitions; an expression prior that ties splice junction usage to promoter methylation in matched tissues. Where priors are made explicit, debiasing becomes possible; where they remain implicit, integration risks becoming a euphemism for averaging incompatible evidence. [52]

Debates persist around what it means to be technology agnostic. A strict reading forbids platform-specific tuning and insists on identical pipelines across inputs, a position that confuses fairness with blindness. A better stance demands invariance at the level of posterior interpretation and loss while granting each channel an optimizer that respects its physics. Equalizing misclassification risk across ancestry groups or sample classes becomes the artifact-free goal, not equalizing read lengths or identical filtering rules. Benchmarks then include stratified truth setssegmental duplications, immunoglobulin loci, GC extremesalongside routine regions, and scoring reports uncertainty as well as accuracy, since equal mean performance with unequal variance distributes risk inequitably across patients.

As devices improve, raw signal fidelity will rise incrementally. Photophysics push fluorophores closer to shot-noise limits; pore engineering separates k-mer states more cleanly; polymerases gain processivity. Gains of this kind move the frontier, yet experience shows that translation into robust assays depends more on the vigor of model validation and standardization [53]. Without shared raw-signal repositories, long-horizon calibration sets, and portable uncertainty representations, improved channels do not guarantee improved inference when deployed outside the training domain. Community infrastructuretruth genomes with challenging structures, open layouts for pangenome graphs, exchange formats for kinetic and current tracesdetermines

the slope at which chemistry becomes biology.

Two concrete implications close the loop from theory to practice. First, design studies around the loss you actually incur if wrong, stated at the level of biological conclusions rather than devices. If a misspecified haplotype would send a patient down an ineffective therapy path, weight phase-preserving channels accordingly and budget for orthogonal confirmation; if a miscounted single nucleotide variant marginally perturbs a polygenic risk score, put more weight on cohort size and calibration stability. Second, treat sample preparation and metadata capture as parameters in the channel, not as preamble. Fragmentation distributions, damage signatures, extraction kits, and storage histories belong in the prior, and decoders should be conditioned on them explicitly through stratified calibration curves or mixture-of-experts basecallers. Neglect here propagates into posteriors whose apparent precision masks brittle assumptions. [54]

Conflict of interest

Authors state no conflict of interest.

References

[1] T. Gould, T. I. Jones, and P. L. Jones, "Precise epigenetic analysis using targeted bisulfite genomic sequencing distinguishes fshd1, fshd2, and healthy subjects.," *Diagnostics (Basel, Switzerland)*, vol. 11, no. 8, pp. 1469–, Aug. 13, 2021. DOI: 10.3390/diagnostics11081469

[2] M. Li et al., "Genomic erbb2/erbb3 mutations promote pd-l1-mediated immune escape in gallbladder cancer: A whole-exome sequencing analysis.," *Gut*, vol. 68, no. 6, pp. 1024–1033, Jun. 28, 2018. DOI: 10.1136/gutjnl-2018-316039

[3] V. J. Carabetta, K. Esquilin-Lebron, E. Zelzion, and J. M. Boyd, "Genetic approaches to uncover gene products involved in iron-sulfur protein maturation: High-throughput genomic screening using transposon sequencing.," *Methods in molecular biology (Clifton, N.J.)*, vol. 2353, pp. 51–68, Jul. 23, 2021. DOI: 10.1007/978-1-0716-1605-5_3

[4] J. Kim et al., "Cryptic genomic lesions in adverse-risk acute myeloid leukemia identified by integrated whole genome and transcriptome sequencing," *Leukemia*, vol. 34, no. 1, pp. 306–311, Aug. 21, 2019. DOI: 10.1038/s41375-019-0546-1

[5] M. D. Stachler and A. J. Bass, "Can genomic sequencing identify high-risk barretts esophagus earlier than pathologists?" *Cancer cell*, vol. 38, no. 5, pp. 626–628, Nov. 9, 2020. DOI: 10.1016/j.ccell.2020.10.020

[6] L. Guo, H. Yao, B. S. Shepherd, O. J. Sepulveda-Villet, D.-C. Zhang, and H.-P. Wang, "Development of a genomic resource and identification of nucleotide diversity of yellow perch by rad sequencing," *Frontiers in genetics*, vol. 10, pp. 992–992, Oct. 14, 2019. DOI: 10.3389/fgene.2019.00992

[7] L. Zhang et al., "Performance of afirma genomic sequencing classifier vs gene expression classifier in bethesda category iii thyroid nodules: An institutional experience.," *Diagnostic cytopathology*, vol. 49, no. 8, pp. 921–927, May 22, 2021. DOI: 10.1002/dc.24765

[8] R. Cristescu et al., "Concordance between single-nucleotide polymorphism-based genomic instability assays and a next-generation sequencing-based homologous recombination deficiency test.," *BMC cancer*, vol. 22, no. 1, pp. 1310–, Dec. 14, 2022. DOI: 10.1186/s12885-022-10197-z

[9] K. He et al., "Functional genomics study of protein inhibitor of activated stat1 in mouse hippocampal neuronal cells revealed by rna sequencing.," *Aging*, vol. 13, no. 6, pp. 9011–9027, Mar. 24, 2021. DOI: 10.18632/aging.202749

[10] Z. Yang, J. Slone, and T. Huang, "Next-generation sequencing to characterize mitochondrial genomic dna heteroplasmy.," *Current protocols*, vol. 2, no. 5, e412–, May 9, 2022. DOI: 10.1002/cpz1.412

[11] L. F. Li, S. A. Cushman, Y. X. He, and Y. Li, "Genome sequencing and population genomics modeling provide insights into the local adaptation of weeping forsythia," *Horticulture research*, vol. 7, no. 1, pp. 130–130, Aug. 1, 2020. DOI: 10.1038/s41438-020-00352-7

[12] T.-T. Pham et al., "Second periprosthetic joint infection caused by streptococcus dysgalactiae: How genomic sequencing can help defining the best therapeutic strategy.," *Frontiers in medicine*, vol. 7, pp. 53–53, Feb. 21, 2020. DOI: 10.3389/fmed.2020.00053

[13] M. J. Cummings et al., "Precision surveillance for viral respiratory pathogens: Virome capture sequencing for the detection and genomic characterization of severe acute respiratory infection in uganda.," *Clinical infectious diseases : an official publication of the Infectious Diseases Society of America*, vol. 68, no. 7, pp. 1118–1125, Aug. 7, 2018. DOI: 10.1093/cid/ciy656

[14] S. D. Grosse and J. M. Gudgeon, "Cost or price of sequencing? implications for economic evaluations in genomic medicine.," *Genetics in medicine : official journal of the American College of Medical Genetics*, vol. 23, no. 10, pp. 1833–1835, Jun. 10, 2021. DOI: 10.1038/s41436-021-01223-9

[15] R. Li et al., "Comprehensive genomic investigation of coevolution of mcr genes in escherichia coli strains via nanopore sequencing.," *Global challenges (Hoboken, NJ)*, vol. 5, no. 3, pp. 2 000 014–2 000 014, Jan. 12, 2021. DOI: 10.1002/gch2.202000014

[16] H. S. Smith, E. S. Bonkowski, M. R. Hickingbotham, R. B. Deloge, and S. Pereira, "Framing the family: A qualitative exploration of factors that shape family-level experience of pediatric genomic sequencing.," *Children (Basel, Switzerland)*, vol. 10, no. 5, pp. 774–774, Apr. 25, 2023. DOI: 10.3390/children10050774

[17] M. Weerakoon, S. Lee, E. Mitchell, and H. Heaton, "Topoqual polishes circular consensus sequencing data and accurately predicts quality scores," *BMC bioinformatics*, vol. 26, no. 1, p. 17, 2025.

[18] R. Hart et al., "Correction: Secondary findings from clinical genomic sequencing: Prevalence, patient perspectives, family history assessment, and health-care costs from a multisite study (genetics in medicine, (2019), 21, 5, (1100-1110), 10.1038/s41436-018-0308-x)," *Genetics in medicine : official journal of the American College of Medical Genetics*, vol. 21, no. 5, pp. 1261–1262, Oct. 5, 2018. DOI: 10.1038/s41436-019-0440-2

[19] K. M. Porter et al., "Approaches to carrier testing and results disclosure in translational genomics research: The clinical sequencing exploratory research consortium experience.," *Molecular genetics & genomic medicine*, vol. 6, no. 6, pp. 898–909, Aug. 21, 2018. DOI: 10.1002/mgg3.453

[20] D. C. Gemenet et al., "Sequencing depth and genotype quality: Accuracy and breeding operation considerations for genomic selection applications in autopolyploid crops.," *TAG. Theoretical and applied genetics. Theoretische und angewandte Genetik*, vol. 133, no. 12, pp. 3345–3363, Sep. 2, 2020. DOI: 10.1007/s00122-020-03673-2

[21] A. Liacini, T. Morris, S. AlZahrani, L. Mathew, and S. Geier, "Full genomic sequence of the hla-dqb1*04:51 allele identified by next-generation sequencing.," *HLA*, vol. 99, no. 2, pp. 142–144, Aug. 19, 2021. DOI: 10.1111/tan.14397

[22] C. Palaiokostas, M. Kocour, M. Prchal, and R. D. Houston, "Accuracy of genomic evaluations of juvenile growth rate in common carp (cyprinus carpio) using genotyping by sequencing.," *Frontiers in genetics*, vol. 9, pp. 82–82, Mar. 13, 2018. DOI: 10.3389/fgene.2018.00082

[23] H. Ayalew et al., "Genotyping-by-sequencing and genomic selection applications in hexaploid triticale.," *G3 (Bethesda, Md.)*, vol. 12, no. 2, Dec. 13, 2021. DOI: 10.1093/g3journal/jkab413

[24] K. Manickam et al., "Exome and genome sequencing for pediatric patients with congenital anomalies or intellectual disability: An evidence-based clinical guideline of the american college of medical genetics and genomics (acmg).," *Genetics in medicine : official journal of the American College of Medical Genetics*, vol. 23, no. 11, pp. 2029–2037, Jul. 1, 2021. DOI: 10.1038/s41436-021-01242-6

[25] M. R. Keever-Keigher et al., "Genomic insights into pediatric intestinal inflammatory and eosinophilic disorders using single-cell rna-sequencing.," *Frontiers in immunology*, vol. 15, pp. 1 420 208–, Aug. 13, 2024. DOI: 10.3389/fimmu.2024.1420208

[26] J. Park, K. Zayhowski, A. J. Newson, and K. E. Ormond, "Genetic counselors' perceptions of uncertainty in pretest counseling for genomic sequencing: A qualitative study," *Journal of genetic counseling*, vol. 28, no. 2, pp. 292–303, Feb. 11, 2019. DOI: 10.1002/jgc4.1076

[27] K. M. Bowling et al., "Return of non-acmg recommended incidental genetic findings to pediatric patients: Considerations and opportunities from experiences in genomic sequencing.," *Genome medicine*, vol. 14, no. 1, pp. 131–, Nov. 21, 2022. DOI: 10.1186/s13073-022-01139-2

[28] A. Parthasarathy et al., "Selfies and cellfies: Whole genome sequencing and annotation of five antibiotic resistant bacteria isolated from the surfaces of smartphones, an inquiry based laboratory exercise in a genomics undergraduate course at the rochester institute of technology.," *Journal of genomics*, vol. 7, pp. 26–30, Feb. 19, 2019. DOI: 10.7150/jgen.31911

[29] L. Cai, Y. Wu, and J. Gao, "Deepsv: Accurate calling of genomic deletions from high-throughput sequencing data using deep convolutional neural network," *BMC bioinformatics*, vol. 20, no. 1, pp. 665–665, Dec. 12, 2019. DOI: 10.1186/s12859-019-3299-y

[30] C. Mighton et al., "Development of patient profiles to tailor counseling for incidental genomic sequencing results," *European journal of human genetics : EJHG*, vol. 27, no. 7, pp. 1008–1017, Mar. 8, 2019. DOI: 10.1038/s41431-019-0352-2

[31] S. Pereira et al., "Perceived benefits, risks, and utility of newborn genomic sequencing in the babyseq project.," *Pediatrics*, vol. 143, no. Suppl 1, S6–S13, Jan. 1, 2019. DOI: 10.1542/peds.2018-1099c

[32] K. A. McCullor, P. B, M. Rahman, C. King, and W. M. McShan, "Genomic sequencing of high-efficiency transducing streptococcal bacteriophage a25: Consequences of escape from lysogeny.," *Journal of bacteriology*, vol. 200, no. 23, Nov. 6, 2018. DOI: 10.1128/jb.00358-18

[33] W. Li, H. Riday, C. Riehle, A. Edwards, and R. D. Dinkins, "Identification of single nucleotide polymorphism in red clover (trifolium pratense l.) using targeted genomic amplicon sequencing and rna-seq.," *Frontiers in plant science*, vol. 10, pp. 1257–, Oct. 23, 2019. DOI: 10.3389/fpls.2019.01257

[34] W. Bahaj, L. Kujtan, O. M. Toor, S. Morris, A. Masood, and J. Subramanian, "Comprehensive genomic analysis of solid tumors by next-generation sequencing.," *Journal of Clinical Oncology*, vol. 36, no. 15$_suppl$, e24291–e24291, May 20, 2018. DOI: 10.1200/jco.2018.36.15_suppl.e24291

[35] S. Prajapati et al., "Genomic sequencing and neutralizing serological profiles during acute dengue infection: A 2017 cohort study in nepal.," *PLOS global public health*, vol. 4, no. 11, e0002966–e0002966, Nov. 13, 2024. DOI: 10.1371/journal.pgph.0002966

[36] A. C. Nelson and S. Yohe, "Cancer whole-genome sequencing: The quest for comprehensive genomic profiling in routine oncology care.," *The Journal of molecular diagnostics : JMD*, vol. 23, no. 7, pp. 784–787, May 18, 2021. DOI: 10.1016/j.jmoldx.2021.05.004

[37] N. A. Pennell et al., "Economic impact of next generation sequencing vs sequential single-gene testing modalities to detect genomic alterations in metastatic non-small cell lung cancer using a decision analytic model.," *Journal of Clinical Oncology*, vol. 36, no. 15$_suppl$, pp. 9031–9031, May 20, 2018. DOI: 10.1200/jco.2018.36.15_suppl.9031

[38] L. Fattel, B. Panossian, T. Salloum, E. Abboud, and S. Tokajian, "Genomic features of vibrio parahaemolyticus from lebanon and comparison to globally diverse strains by whole-genome sequencing.," *Foodborne pathogens and disease*, vol. 16, no. 11, pp. 778–787, Jul. 8, 2019. DOI: 10.1089/fpd.2018.2618

[39] D. T. Miller et al., "Correction to: Acmg sf v3.0 list for reporting of secondary findings in clinical exome and genome sequencing: A policy statement of the american college of medical genetics and genomics (acmg).," *Genetics in medicine : official journal of the American College of Medical Genetics*, vol. 23, no. 8, pp. 1582–1584, May 20, 2021. DOI: 10.1038/s41436-021-01278-8

[40] H. S. Smith et al., "Perceived utility of genomic sequencing: Qualitative analysis and synthesis of a conceptual model to inform patient-centered instrument development.," *The patient*, vol. 15, no. 3, pp. 317–328, Oct. 18, 2021. DOI: 10.1007/s40271-021-00558-4

[41] M. J. Riggs et al., "Factors predicting participation in the prospective genomic sequencing study, total cancer care (tcc), in kentucky," *The Journal of rural health : official journal of the American Rural Health Association and the National Rural Health Care Association*, vol. 38, no. 1, pp. 5–13, Jul. 6, 2020. DOI: 10.1111/jrh.12492

[42] B. Yuan et al., "Sequencing individual genomes with recurrent genomic disorder deletions: An approach to characterize genes for autosomal recessive rare disease traits.," *Genome medicine*, vol. 14, no. 1, pp. 113–, Sep. 30, 2022. DOI: 10.1186/s13073-022-01113-y

[43] I. Griesemer et al., "Engaging community stakeholders in research on best practices for clinical genomic sequencing.," *Personalized medicine*, vol. 17, no. 6, pp. 435–444, Oct. 7, 2020. DOI: 10.2217/pme-2020-0074

[44] R. Guo et al., "Genomic prediction of kernel zinc concentration in multiple maize populations using genotyping-by-sequencing and repeat amplification sequencing markers.," *Frontiers in plant science*, vol. 11, pp. 534–, May 8, 2020. DOI: 10.3389/fpls.2020.00534

[45] H. Chen et al., "Epidemiological and whole genomic sequencing analysis of a campylobacter jejuni outbreak in zhejiang province, china, may 2019.," *Foodborne pathogens and disease*, vol. 17, no. 12, pp. 775–781, Jul. 7, 2020. DOI: 10.1089/fpd.2020.2794

[46] L. M. Amendola et al., "The clinical sequencing evidence-generating research consortium: Integrating genomic sequencing in diverse and medically underserved populations," *American journal of human genetics*, vol. 103, no. 3, pp. 319–327, Sep. 6, 2018. DOI: 10.1016/j.ajhg.2018.08.007

[47] W. M. Ismail and H. Tang, "Clonal reconstruction from time course genomic sequencing data," *BMC genomics*, vol. 20, no. 12, pp. 1–11, Dec. 30, 2019. DOI: 10.1186/s12864-019-6328-3

[48] T. C. Borelli et al., "Combining functional genomics and whole-genome sequencing to detect antibiotic resistance genes in bacterial strains co-occurring simultaneously in a brazilian hospital," *Antibiotics (Basel, Switzerland)*, vol. 10, no. 4, pp. 419–, Apr. 11, 2021. DOI: 10.3390/antibiotics10040419

[49] D. F. Stiles and P. S. Appelbaum, "Cases in precision medicine: Concerns about privacy and discrimination after genomic sequencing.," *Annals of internal medicine*, vol. 170, no. 10, pp. 717–721, May 7, 2019. DOI: 10.7326/m18-2666

[50] R. Huether et al., "A comprehensive whole genome sequencing assay provides robust characterization of clinically relevant genomic alterations across myeloid malignancies concordant with matched results from targeted dna, whole transcriptome rna and cytogenetic profiling," *Blood*, vol. 144, no. Supplement 1, pp. 7481–7481, Nov. 5, 2024. DOI: 10.1182/blood-2024-199194

[51] E. A. C. Heath-Heckman and M. K. Nishiguchi, "Leveraging short-read sequencing to explore the genomics of sepiolid squid.," *Integrative and comparative biology*, vol. 61, no. 5, pp. 1753–1761, Jun. 30, 2021. DOI: 10.1093/icb/icab152

[52] R. N. Lou, A. Jacobs, A. P. Wilder, and N. O. Therkildsen, "A beginner's guide to low-coverage whole genome sequencing for population genomics.," *Molecular ecology*, vol. 30, no. 23, pp. 5966–5993, Aug. 31, 2021. DOI: 10.1111/mec.16077

[53] M. Parker et al., "Subgenomic rna identification in sars-cov-2 genomic sequencing data.," *Genome research*, vol. 31, no. 4, pp. 645–658, Mar. 15, 2021. DOI: 10.1101/gr.268110.120

[54] O. M. Toor et al., "Correlation of somatic genomic alterations between tissue genomics and ctdna employing next-generation sequencing: Analysis of lung and gastrointestinal cancers.," *Molecular cancer therapeutics*, vol. 17, no. 5, pp. 1123–1132, Apr. 30, 2018. DOI: 10.1158/1535-7163.mct-17-1015